Performance evaluation of a novel concept "Open Plate Reactor" applied to highly exothermic reactions

Laurent Prat, Audrey Devatine, Patrick Cognet, Michel Cabassud, Christophe Gourdon, Sébastien Elgue, Fabrice Chopard

Performance evaluation of a novel concept “open plate reactor” applied to highly exothermic reactions

L. Prat, A. Devatine, P. Cognet, M. Cabassud, C. Gourdon
Laboratoire de Génie Chimique (UMR 5503), CNRS-INPT-UPS
B.P. 1301, 5 rue Paulin Talabot, 31106 Toulouse Cedex 1, France

S. Elgue, F. Chopard
Alfa Laval Vicarb
B.P. 200, 38522 Saint Egrève Cedex, France

Abstract : The implementation of chemical reactions in batch or semi-batch reactors is strongly limited by the constraints linked to the dissipation of the heat generated by the reactions. The novel concept of heat exchanger reactors offers enhanced thermal performances in a continuously operating reactor. A study program is proposed to assess the feasibility and potentialities of this novel concept.
Two kinds of reactions are carried out to characterize simultaneously the reactor performances in terms of reaction and heat exchange: the oxidation of sodium thiosulfate by hydrogen peroxide and an acido-basic reaction ($NaOH/H_2SO_4$).
The resultant experimental data emphasize a significant thermal efficiency : the reactant concentrations and therefore the heat generation can be increased without risk of thermal runaway.

Keywords: process intensification, chemical reactor, continuous multifunctional reactor, exothermic reactions, heat exchanger

1. INTRODUCTION

Most of the production of fine chemicals is operated in multifunctional reactors, usually stirred tank reactors in semi-batch mode. Stirred tank reactors are reliable and flexible to the demands of multifunctional plants, but the scale up from lab to production is difficult. Furthermore, the low ratio between the heat exchange area and the reaction volume forces to consider diluted systems or slow feeding in order to adapt the reaction kinetics to the thermal constraints (1).
This statement has led research teams to design and develop new devices based on the coupling of high heat transfer performances and good mixing. Among them, the HEX reactor (2, 3) , the OBR (4) or reactors using static mixer technologies (5).
The present work is devoted to the characterization of the chemical and thermal performances of a novel intensified reactor: the OPR (Open Plate Reactor) designed by Alfa Laval Vicarb.

2. PILOT AND OPERATION DESCRIPTION

2.1 Pilot description

The reactor is composed of 3 blocks implemented in a plate heat exchanger made of 6 sandwich plates. The thermal flow configuration is not the same all along the reactor: co-current for both first and third blocks and counter-current for second block (Figure 1). A computer-controlled valve regulates the utility flow rate (F_u^{in}) in a 0 to 3.5 $m^3.h^{-1}$ range. This flow rate is measured with an electromagnetic flowmeter. The reactor can be supplied with 3 different fluids (raw water, cold water and hot oil) inside a temperature range of 13°C to 140°C.

Two feed lines are available for the process fluid and there is one outlet product line. The feed lines ensure reactant introduction in the reactor at a given temperature (T_p^{in}): the main line has a nominal operating point of 40 $L.h^{-1}$ (F_{p1}^{in}), while the secondary line operates at 10 $L.h^{-1}$ (F_{p2}^{in}). Each line includes a pump and a flow rate measurement system. Two different flowmeter technologies have been used. For conductive liquids, an electromagnetic flowmeter has been chosen while, for non-conductive liquids, a Coriolis flowmeter is used.

At the reactor outlet, a valve is disposed on the product line to adjust the pressure inside the reactor (P_p^{out}).

Temperature measurement facilities (PT100) are set up on inlet and outlet lines for reagents, product (T_p^{in} and T_p^{out}), and utility lines (T_u^{in} and T_u^{out}). At the output of the first block, product line and utility temperatures are available (respectively $T_p^{first\ block}$ and $T_u^{first\ block}$). Furthermore, eight thermocouples, listed from A to H, are implemented along the first block in order to provide a temperature profile (T_p^A to T_p^H). Table 1 gives these thermocouples locations.

Pressure measurement devices are set up on utility line inlet and on all lines of the process fluid.

All measurements are recorded by an on-line data storage system.

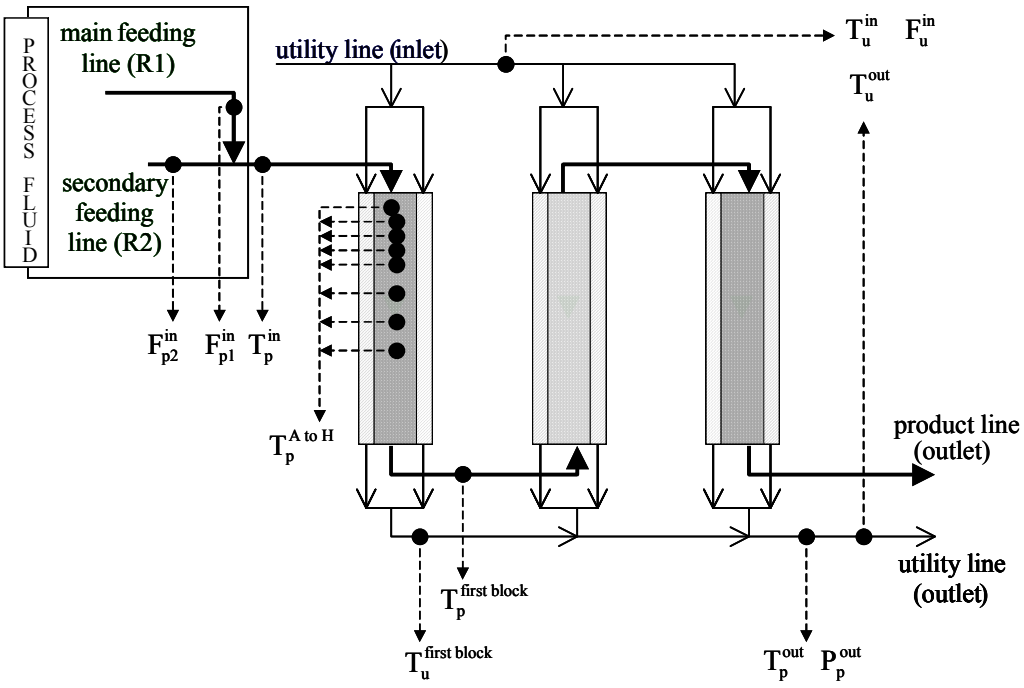

Figure 1. Pilot plant and measurements

	Traversed Volume (L)	Time to reach thermocouple at 50 $L.h^{-1}$ (s)
T_p^A	0.0237	1.7
T_p^B	0.0405	2.9
T_p^C	0.0573	4.1
T_p^D	0.0909	6.5
T_p^E	0.1747	12.6
T_p^F	0.2586	18.6
T_p^G	0.3425	24.7
T_p^H	0.4264	30.7
$T_p^{first\ block}$	0.4600	33.1
$T_p^{second\ block}$	0.9200	66.2
T_p^{out}	1.3800	99.3

Table 1. Sensor locations along the OPR on the process fluid

In the studied configuration, the maximum residence time is 100 s, but this time can be easily increased by adding supplementary blocks.

2.2 Start-up procedure

Cooling fluid is supplied one hour before the beginning of an experiment in order to thermostat the metallic part of the reactor. Reactions are usually carried out with an excess of one reactant, this latter being firstly introduced in the reactor, already filled up of distilled water.
Problem of air bubbles in the process fluid line inside the reactor is a difficult problem to tackle. A special procedure has been defined to eliminate and cope with this problem: for each experiment, the pressure profile is monitored while the flow rate of the main feed line decreases over time then increases again until its nominal value (time of each test is about 20 min). If the obtained curve presents hysteresis, it indicates air bubble presence and the reactor is purged again. All experiments are performed in a purged reactor
When steady state is reached (all temperatures appear stable), the second reactant is injected. At the outlet of the reactor, a sampling device allows checking the value of the conversion by analysis. The flow rates of reagents are fixed to 40 $L.h^{-1}$ and 10 $L.h^{-1}$ respectively.

3. EXPERIMENTAL RESULTS

3.1 Residence time distribution experiments

RTD experiments have been carried out to characterize the process fluid behaviour in the OPR, using two conductivity probes. The first one is located at the tracer (KOH solution) injection point. In all experiments, the first probe gives a dirac signal and this will be the retained hypothesis for all the RTD analysis. The second probe is at the outlet of the reactor.

For each RTD, experiment has been performed at room temperature, with water used as process fluid. The process flow rates were respectively for main and secondary line: 40-10 and 20-5 $L.h^{-1}$.

Figure 2 presents the RTD obtained with the two different flow rates. All the experimental curves have been represented using a reduced time variable.

The curves indicate a relative good plug-flow behaviour (especially for the RTD done at the nominal functioning point (a)). Curve (b) with 20-5 L.h-1 presents a longer tail at the end of the signal. This is certainly due to the presence of recirculation flows in the angles.

These experimental results are in a good agreement with the observations and calculations done by Bouaifi & al. (6). It has been noticed that the channel reactor contains mixing elements arranged in series. This specific design offers a good mixing performances by constantly changing the direction of

the flow. This allows to increase shear rates and turbulence generation and dissipation (6). Finally, we can consider that for nominal operating conditions a plug flow behaviour can be assured.

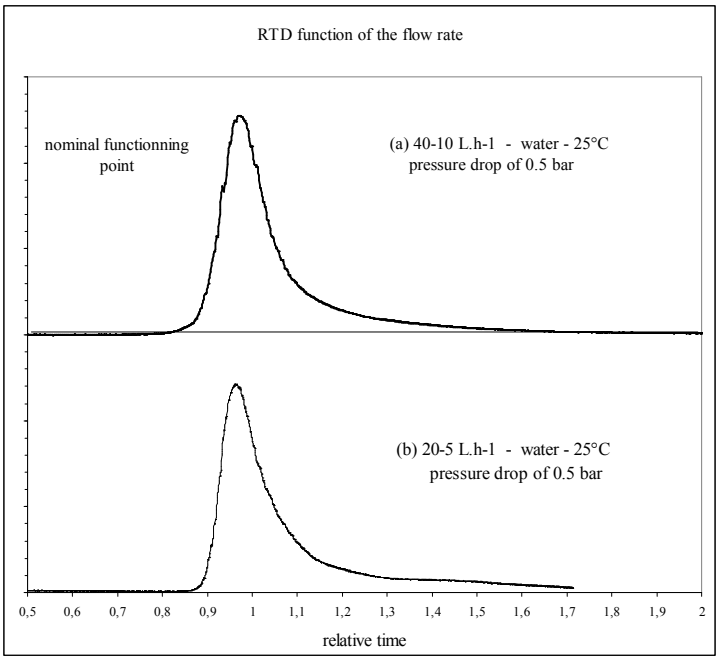

Figure 2 : RTD function of the flow rate or the pressure drop

3.2 Thermal characterisation

The heat exchanged during the process is computed using data collected from the process fluid (flow rate and temperature variation).

On the process fluid, the global heat exchanged (kW) is defined according to the following equation:

$$Q_{global} = F_p^{in} \,.\, C_p \,.\, \left(T_p^{out} - T_p^{in} \right) + Q_{generated} \qquad \text{(heat balance on the reactor)} \qquad \text{(eq 1)}$$

and $$Q_{generated} = w_i \cdot F_{p_i}^{in} \cdot \Delta H_{Ri} \qquad \text{(reaction heat balance)} \qquad \text{(eq 2)}$$

where w_i and F_{pi}^{in} (mass concentration and flow rate) are related to the limitant reagent.

In the case of an instantaneous exothermic reaction, we can assume that all the reaction heat is generated at the very beginning of the first block. Considering a position where the process fluid temperature has not yet reach the corresponding utility temperature, it is possible to calculate a global heat transfer coefficient U with equation 3:

$$U = \frac{Q_{position}}{A \cdot \Delta T_{lm}} \qquad \text{(global heat transfer coefficient)} \qquad \text{(eq 3)}$$

with

$$Q_{position} = F_p^{in} \,.\, C_p \,.\, \left(T_p^{position} - T_p^{in} \right) + Q_{generated} \qquad \text{(heat balance on the first block)} \qquad \text{(eq 4)}$$

and

$$\Delta T_{lm} = \frac{\left(T_p^{in\prime} - T_u^{in}\right) - \left(T_p^{position} - T_u^{position}\right)}{\ln \frac{\left(T_p^{in\prime} - T_u^{in}\right)}{\left(T_p^{position} - T_u^{position}\right)}} \qquad \text{(logarithmic-mean temperature difference)} \qquad \text{(eq 5)}$$

As reaction occurs mainly at the very beginning of the first block, the process fluid inlet temperature has been modified with the adiabatic increase of temperature:

$$T_p^{in\prime} = T_p^{in} + \Delta T_{adiabatic} \qquad \text{(correction on the inlet temperature)} \qquad \text{(eq 6)}$$

Due to the high values of the utility flow rates, there is no significant difference between utility inlet and outlet temperature values. Thus, it is not possible to use this information to present heat balances on the utility fluid.

3.2.1 Tests performed with water

First tests have been done with water. Hot water (20 to 60 °C) has been introduced as the process fluid with a 50L.h-1 flow rate, while the inlet utility water was at about 13°C. The utility flow rate varies from 0.21 to 1.25 m3.h-1.

Figure 3 shows an example of the temperatures recording along the OPR during the experiment. At t=77 s, the process fluid starts to circulate inside the reactor. At t=1500 s, the utility flow rate goes from F_u^{in}=0.21 $m^3.h^{-1}$ to 0.88 $m^3.h^{-1}$. As expected, process fluid temperatures decrease along the OPR. In this case, all the thermal exchange is completed when the fluid reaches thermocouple H. Furthermore, the time to reach steady state is about 300 s.

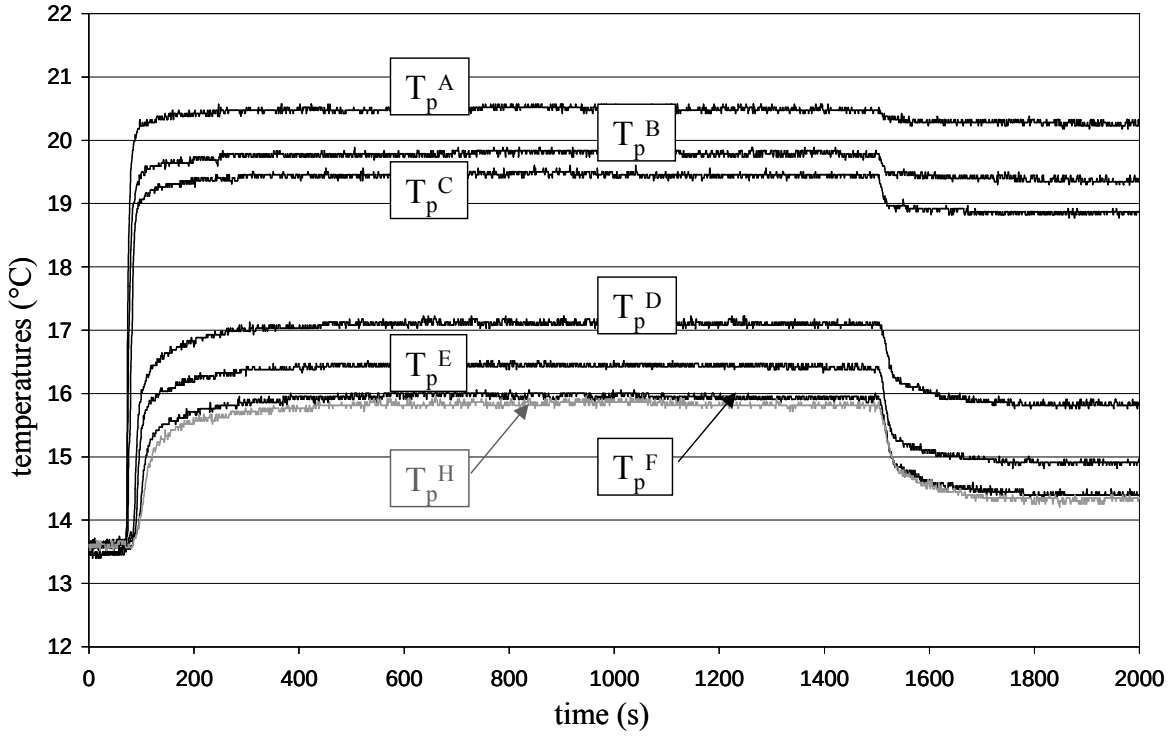

Figure 3 : example of temperatures recording during experiment (T_p^{in}=22°C)

Figure 4 shows the recording of the process fluid temperature of steady state along the reactor for the 1.5 m3.h-1 utility flow rate and for different T_p^{in}.

Considering that the utility temperature does not change along the reactor (i.e. the exchanged heat is low compared to the F_u^{in} . C_{pu} value), the same level of temperature in the process fluid corresponds to the same heat exchanged with the utility fluid. This hypothesis is verified for high utility flow rates as the temperature of this fluid increases up to 2°C along the reactor. For the lowest flow rate (0.21 m3.h-1), the increase in temperature can reach 7°C. This allows to represent the experimental points independently of the process inlet temperature, as shown Figure 5.

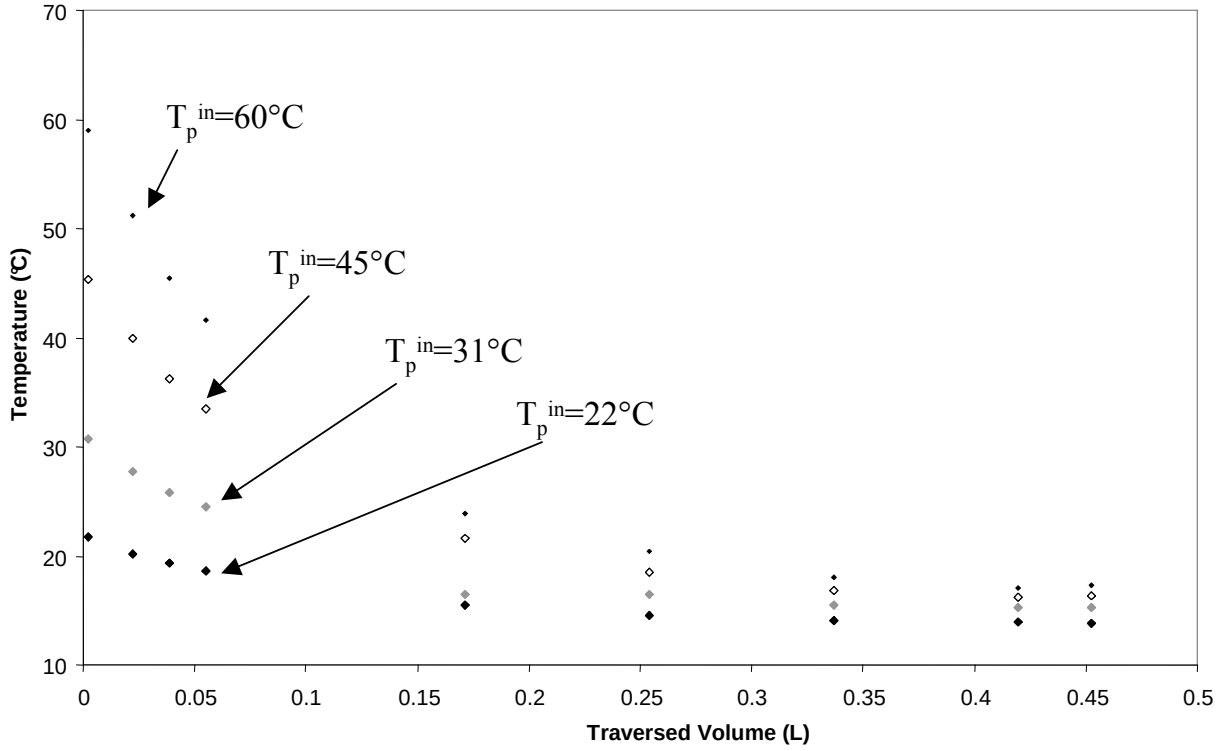

Figure 4 : profile temperatures along the reactor in steady state for different T_p^{in}

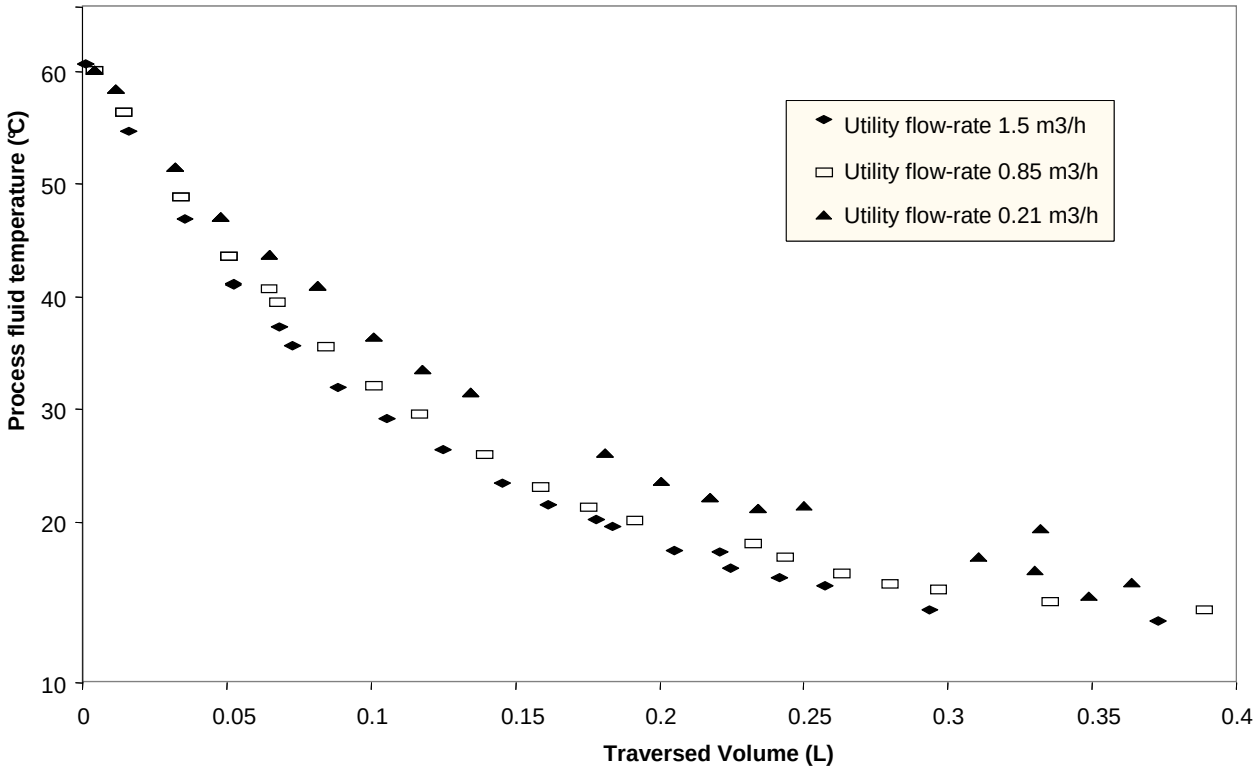

figure 5 : temperatures profile along the reactor

Temperatures decreases along the reactor and this decrease is faster for the higher utility flow rate. For the last times of the fluid in the reactor, the experimental values are more dispersed around a mean value. This is due to the hypothesis made on the utility temperature along the device (the last points of the 0.21 m3.h-1 have no been considered for the next calculations).

From equation 3 and data of Figure 5 it is possible to calculate U, the global heat exchange coefficient. Table 2 presents the experimental results. U varies from 1850 to 2500 $W.m^{-2}.K^{-1}$. These values are intermediary between the coefficients obtained in plate exchangers and than the ones obtained in tubular reactors and far away from values measured in batch reactors.

T_p^{in} (°C)	F_u^{in} ($m^3.h^{-1}$)	T_p^{out} (°C)	U ($W.m^{-2}.K^{-1}$)
60,4	0,22	25,3	1892
60,8	0,88	19,0	2416
60,2	1,52	17,4	2709
44,3	0,21	21,4	1845
44,5	0,87	17,4	2316
43,9	1,47	16,4	2545
31,4	0,20	18,3	1965
30,9	0,80	15,8	2334
30,7	1,40	15,3	2544
21,5	0,21	15,8	1650
22,3	0,86	14,4	2072
22,2	1,50	13,9	2275

Table 2 : global heat transfer coefficient for water experiments

It can be observed that U increases with the utility flow rate and with the initial process fluid temperature. This corresponds to a classical evolution of the Nusselt number, function of the Reynolds and the Prandtl numbers.

3.2.2 Tests with a highly exothermic reaction

These series of experiments focus on the oxidation reaction of sodium thiosulfate $Na_2S_2O_3$ by hydrogen peroxide H_2O_2. The stoechiometric scheme is :

$$2\ Na_2S_2O_3 + 4\ H_2O_2 \rightarrow Na_2S_3O_6 + Na_2S0_4 + 4\ H_2O$$

This liquid homogeneous reaction is irreversible, fast and highly exothermic (7, 8). The kinetics can be described by: $r = k\ [S_2O_3^{2-}].[H_20_2]$
with $k = k°.\exp(-E/RT)$ and $k° = 2.10^{10}$.L. $mol^{-1}s^{-1}$ and $E = 6.82.10^4$ $J.mol^{-1}$.

The reaction heat is ΔHR = - 586,2 $kJ.mol^{-1}$ (- 140 $kcal.mol^{-1}$).

The utility fluid is water. The aqueous sodium thiosulfate is introduced through the main inlet process fluid (40 $L.h^{-1}$). In order to avoid possible side reaction, H_2O_2 is in excess. The maximum weight percent in the inlet flows are 30% for H_2O_2 and 35% for $Na_2S_2O_3$. At this level of concentrations, the salts solubilities can not be reached (9). Furthermore, in order to qualify the interaction between H_2O_2 and the stainless steel of the reactor, the following experiment has been performed: H_2O_2 and water (instead of $Na_2S_2O_3$) are introduced at maximum concentration (30 %w) and at a temperature of 313K. The non evolution of the mass of H_2O_2 between inlet and outlet flows confirms that no side reaction occurs between H_2O_2 and the material of the reactor.

Due to the instability of the products, H_2O_2 and $Na_2S_20_3$ are titrated with potassium dichromate by manganimetry and iodometry respectively before each experiment (10, 11). To determine the conversion rate at the products outlet, a calorimetric method is used. A measured amount of the outlet liquid is fed in an adiabatic cell. The temperature is recorded until the reaction ends. The difference between the initial temperature and the temperature reached at steady state allows to calculate the reaction yield of the experiment:

$$\eta = 1 - \frac{(m.C_p + m_V.C_{pV}).\Delta\theta}{\Delta H_r.V.C_0} \qquad \text{(eq 7)}$$

where m, V are the mass and volume of the sample,
Cp, the specific heat of the sample,
m_V, C_{pV} are the mass and the specific heat of the adiabatic vessel,
$\Delta\theta$, the temperature variation,
C_0 the initial concentration.

Two experiments have been performed, varying the reagents concentrations: the weight percent in the inlet flows are 21.8% for H_2O_2 and 12.3% for $Na_2S_2O_3$ for experiment A and 26.7% for H_2O_2 and 14.2% for $Na_2S_2O_3$ for experiment B. Generated heat is then 5.5 kW for experiment A and 6.6 kW for experiment B.

Temperatures of the inlet process and utility fluids are 13°C.

Figure 6 shows the temperatures recording along the OPR during the experiment A. At t=10 min, reagents are introduced in the OPR. Initial utility flow rate is 0.22 $m^3.h^{-1}$, at 46 min, it goes up to 0,91 $m^3.h^{-1}$ and at 64 min, it is increased to 1.76 $m^3.h^{-1}$. At about 16.5 min, a short variation on the fluid inlet temperature occurs.

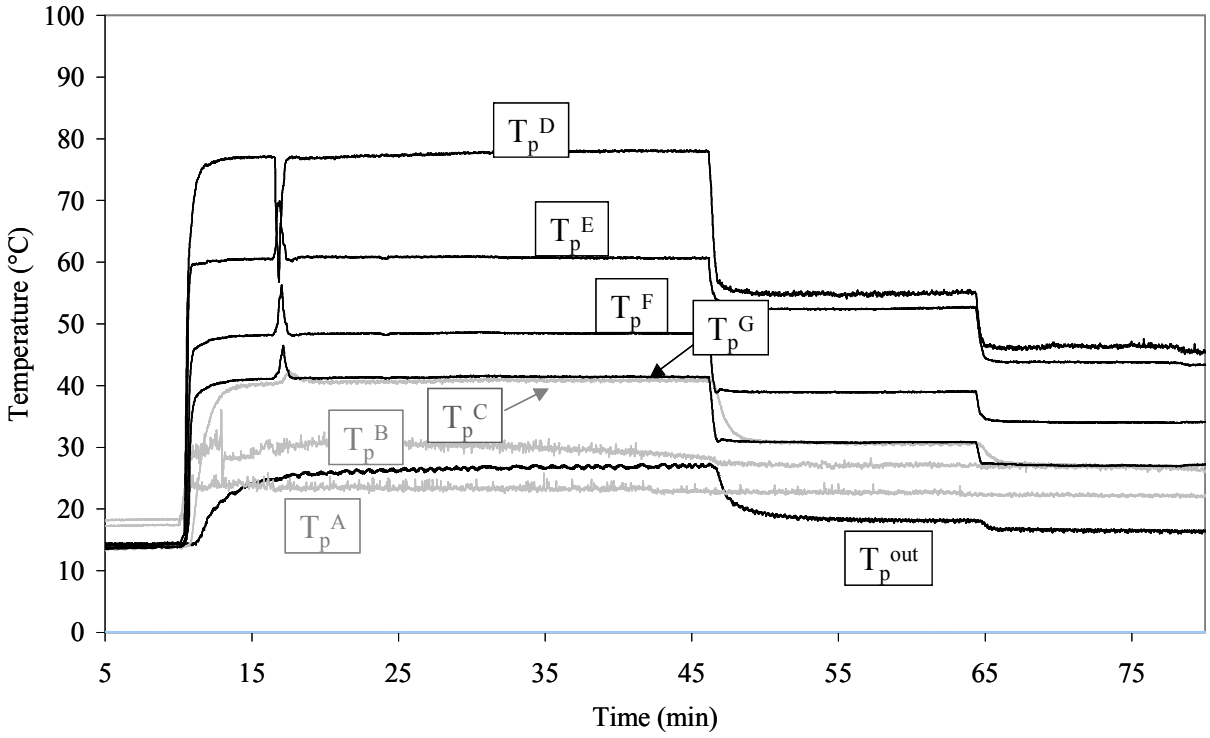

Figure 6 : temperatures recording during oxidation experiment A (T_p^{in}=13°C)

From these experimental results it is possible to represent the temperature profile in the OPR at steady state (Figure 7 for experiment A and Figure 8 for experiment B) and then to calculate the global heat transfer coefficient. In experiment A, due to the short residence time and the level of temperature, the reaction is not totally completed inside the OPR. Of course this should be addressed by simply adding another plate. The measured conversion rates are respectively 100, 95 and 87 % for the 0.22, 0.91 and 1.76 $m^3.h^{-1}$ utility flow rates.

As expected, due to the fast kinetic of the reaction, the process fluid temperatures profile presents a maximum at the beginning of the reactor, and then decreases along the OPR. Furthermore, the step increase in utility flow rate allows to estimate the time necessary to reach steady state at 5 min.

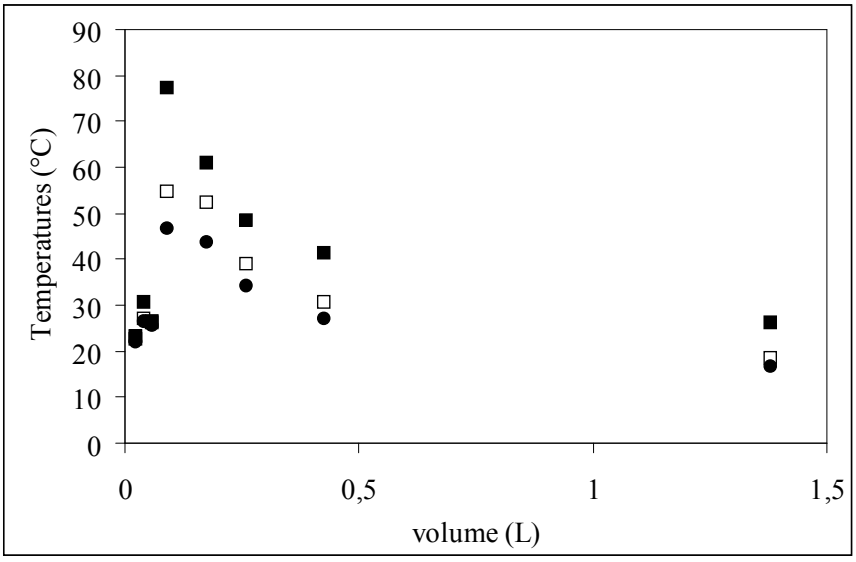

Figure 7 : temperatures profile for oxidation experiment A
(■ for F_u^{in}=0.22 $m^3.h^{-1}$, □ for F_u^{in}=0.91 $m^3.h^{-1}$, ● for F_u^{in}=1.76 $m^3.h^{-1}$)

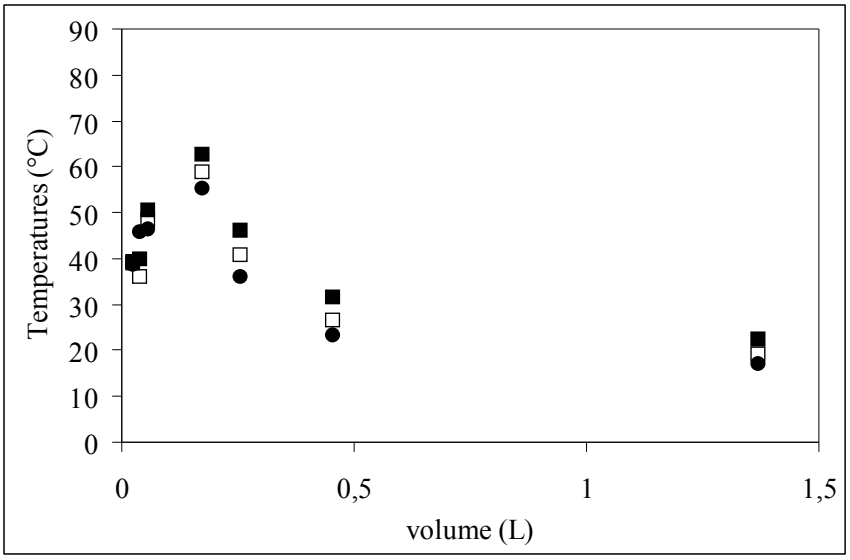

Figure 8 : temperatures profile for oxidation experiment B
(■ for F_u^{in}=0.56 $m^3.h^{-1}$, □ for F_u^{in}=0.85 $m^3.h^{-1}$, ● for F_u^{in}=1.80 $m^3.h^{-1}$)

	Experiment A			Experiment B		
utility flow rate ($m^3.h^{-1}$)	0.22	0.91	1.76	0.56	0.8	1.8
% w. H_2O_2	21.8			26.7		
% w. $Na_2S_2O_3$	12.3			14.2		
Heat generated (kW)	5.5			6.6		
$\Delta T_{adiabatic}$	95			110		
Conversion rate (%)	100	95	87	100		
U ($W.m^{-2}.K^{-1}$)	1430	1788	1926	1464	1625	1760

Table 3 : Experimental conditions and results for oxidation

Table 3 presents the calculated values of the global heat transfer coefficients for the different utility flow rates. As expected, U increases with the utility flow rate. U varies from 1400 to 2000 $W.m^{-2}.K^{-1}$. These values are a little bit smaller then the coefficients obtained for the water experiments. This is due to the calculation. Indeed, the temperature profile at the beginning of the reactor is not considered and then the temperatures are over evaluated. This tends to over evaluate the ΔT_{ml} used in equation 3 and this results in smaller values of U. In order to correct the values of the heat transfer coefficient, a reaction model has to be used and coupled with the heat balance. This will give the conversion yield and then the heat generated along the reactor.
In the presented oxidation, the reagents concentrations could not have been implemented in batch reactor because of the adiabatic temperature. The way to perform such a reaction in stirred tank reactors is to dilute or to feed slowly the reagents.

3.2.3 Tests performed with an instantaneous exothermic reaction

To evaluate the heat exchanged/productivity performances of the device and its environment, an acid-base neutralisation involving sulphuric acid and soda has been performed. It is an instantaneous and exothermic reaction having a reaction heat of ΔH = - 92.4 $kJ.mol^{-1}$ (NaOH). Each experiment is

characterised by the initial concentration of the reactants (from 10 to 30% in mass of soda and from 5 to 12% in mass of sulphuric acid). These concentrations are varied in order to evaluate the behaviour of the reactor with respect to different amounts of generated heat (from 0.4 to 1.3 kW). Each run is performed with a variable utility flow rate (from 1 to 3 $m^3.h^{-1}$).

%w NaOH	%w H_2SO_4	T_p^{in} (°C)	$\Delta T_{adiabatic}$ (°C)	$Q_{generated}$ (kW)	F_u^{in} ($m^3.h^{-1}$)	U ($W.m^{-2}.K^{-1}$)
10,5	5,9	19,4	7,0	0,43	1	1990
10,5	5,9	19,6	6,7	0,41	3	2100
14,6	6,1	18,4	10,1	0,62	1	1970
14,6	6,1	17,5	10,8	0,67	2,8	2194
17,0	6,9	19,7	12,3	0,79	1	2223
27,0	11,7	18,1	19,9	1,28	1	2207
27,0	11,7	18,2	19,6	1,26	3	2469

Table 4 : global heat transfer coefficient for acid/base experiments

Table 4 presents the experimental results. U varies from 1950 to 2500 $W.m^{-2}.K^{-1}$. As expected, U increases with the utility flow rate. These values are in the same order of magnitude of coefficients obtained for the water experiments. In that case, all the reaction occurs at the very beginning of the reactor and so is the heat generated. The hypothesis for equations 3 to 6 are then actually verified.

4. CONCLUSION

This work described the experimental implementation of a novel multifunctional channel reactor designed and built by Alfa Laval Vicarb. It has been instrumented in order to measure at the inlet and at the outlet the characteristics of the utility and the process flows. Furthermore, thermocouples have been implemented in order to obtain a temperature profile inside the reactor.
Based on RTD experiments and on acid/base and oxidation experiments it has been possible to characterize this apparatus in a global point of view. The behaviour of the process flow tends towards a plug flow with good reagents mixing at the nominal functioning point.
Heat transfer coefficients calculated from the experiments vary in a 1950 to 2500 $W.m^{-2}.K^{-1}$ range.
In the case of non instantaneous reactions, the next step of this study will be to introduced in the calculation the kinetic and the conversion along the reactor.

These characteristics make this apparatus very interesting as it is a good balance between a reaction and a heat transfer dedicated apparatus.

Compared to microstructured reactor-heat exchanger, the OPR presents one specific characteristic: the process fluid circulates in one continuous channel which offers a 0.5 cm2 cross section. Compared to other devices based on plate exchanger or static mixers design, the OPR has a lower ratio between heat exchange surface/reaction volume.
But this structure will allow the use of viscous media or in certain conditions solid-liquid or liquid-liquid media. Furthermore, it is possible to introduce and quickly mix in any location of the channel (i.e. at any time) new reagents and then implement complex multi-step reactions.

This novel reactor is then a promising apparatus for fast and highly exothermic systems, allowing to work in non classical temperatures and concentrations domain (indeed, due to heat transfer constraints, high temperatures and high concentrations are not often studied in standard reactors). This opportunity to function with high concentrations and then high kinetics compensates the low residence time of each block.

Acknowledgement
This work was financially supported by Alfa Laval Vicarb AB (Process Technology Division) and the INPT/UPS/CNRS.

REFERENCES

(1) Stitt E.H., Alternative multiphase reactors for fine chemicals: a world beyond stirred tanks?, Chemical Engineering Journal, 90, 47-60, 2002.
(2) Riley C.J. et Phillips C. H., Benefits of using integrated chemical reactor- heat exchangers (HEX reactors) in the Dutch chemical industry, BHR-6858. BHR Group, 18 August 1998, Cranfield, U.K.
(3) Phillips C.H., G. Lauschket and H. Peerhossaini, Intensification of batch chemical processes by using integrated chemical reactor-heat exchangers, Applied Thermal Engineering 17 n°8-10 (1997) 809-824.
(4) Xiog-Wei Ni, Fitchand A., Webster P., From a maximum to most efficient production using a continuous oscillatory baffled reactor, Centre for Oscillatory Baffled Reactor Applications (COBRA), Chemical Engineering, School of Engineering and Physical Sciences, Heriot-Watt University, Edinburgh, EH144AS, UK.
(5) Brechtelsbauer C., Ricard F., Reaction Engineering Evaluation and Utilization of Static Mixer Technology for the Synthesis of Pharmaceuticals, Organic Process Research and Development, 5, (2001) 646-651.
(6) Bouaifi M., Mortensen M., Andersson R., Orciuch W. Andersson B., Chopard F., Noren T., Experimental and numerical investigations of a jet mixing in a multifunctional channel reactor : passive and reactive systems, Trans IChemE, Part A, Chemical Engineering Research and Design, 2004, 82(A2): 274–283
(7) Lo S.N., Cholette A., Effect of channelling on the performance of adiabatic flow tank reactors for exothermic reactions, Canadian Journal of Chemical Engineering, 50(1), 66-70, 1972.
(8) Lo S.N., Cholette A., Experimental study on the optimum performance of an adiabatic MT reactor, Canadian Journal of Chemical Engineering, 50(1), 71-80, 1972.
(9) Lide D. R., Handbook of chemistry and physics, 80e ed., Ed. Boca Raton , Crc press, 1999.
(10) Barthel J., Schmahl N.G., Thermometric redox titration, Zeitschrift für Analytische Chemie, 207(2), 81,90, 1965.
(11) Funk E. H., Herlinger A. W. , Convenient preparation of standard thiosulfate solutions, Analytical Chemistry, 47(4), 767-8, 1975.